22

Composite Material for Shielding Mixed Radiation

Hu Huasi
School of Nuclear Science and Technology, Xi'an Jiaotong University (XJTU), Xi'an, 710049 Shannxi, China

1. Introduction

1.1 Composite material design idea for shielding mixed radiation

What we have done is to design a shielding material of high performance secures us or nuclear facilities from radiation. However, most of you are unfamiliar with nuclear physics, so here you may consider the nuclear radiation shielding, the transportation of neutrons and other particles in material, as small balls with velocity rolling on the surface of Mars. Admittedly, this hypothesis is questionable, but it may prepare you for understanding. Now, we take neutron transportation as an example. In left of Fig.1, Twenty small bolls of high speed (fast neutrons) roll towards right on Mars. Some of them, three or more, trapped by hollows disappear, the others have collided against the rocks scatter with lower energy, only a few of them may go across holding tiny energy (thermal neutrons). Nuclear reaction cross sections determine probability of trapping and collision.

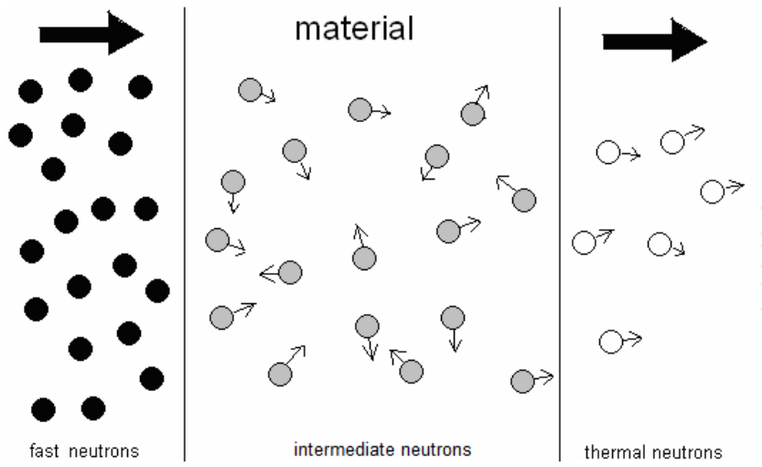

Fig. 1. The transportation of neutrons in material

This work was supported by the National Natural Science Foundation of China (Grant No.10576022, 10975113), the National High Technology Research and Development Program of China (Grant No.2009AA050705), and NINT Contract 200509006.
E-mail: huasi_hu@mail.xjtu.edu.cn

The following picture Fig.2 is the brief interaction of neutrons with other materials. The heavy metal elements, such as tungsten and iron, slow down the fast neutron to intermediate neutron by the inelastic scattering and resonance scattering; then, the low-Z elements by elastic scattering cool the intermediate neutron down into the thermal neutron group. Finally some elements such as boron capture the thermal neutrons. The high-Z elements absorb both original and secondary γ-rays.

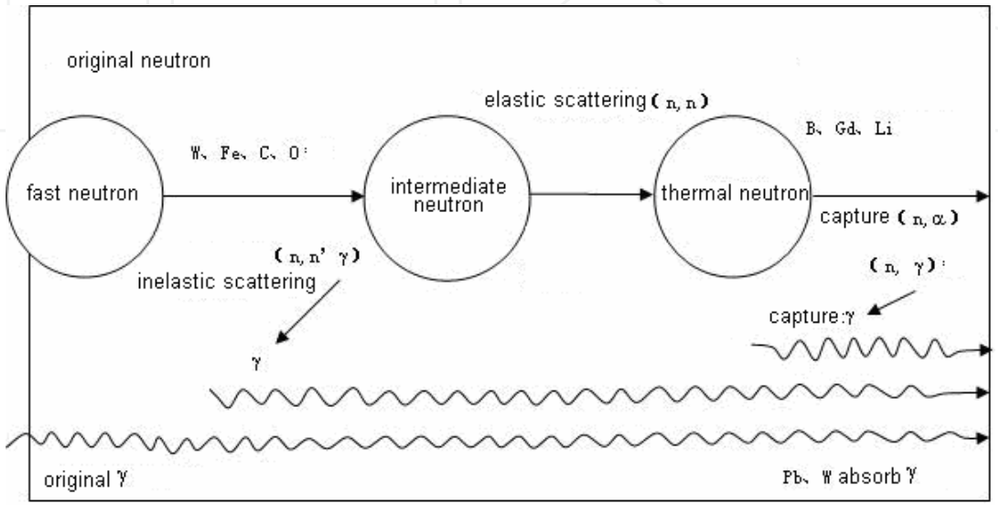

Fig. 2. The brief interaction mechanism

Nowadays, many kinds of materials were employed as nuclear radiation shielding material, while, the requirements of radiation shielding become more and more strictly. Especially in mobile nuclear devices and manned spacecrafts [1][2], the radiation shielding materials must have high effective shielding properties for the sake of the restriction the materials' weight and volume. Also, shielding materials have to service for a long time in quite inclement environment with high temperature, corrosion, and so on. Furthermore, shielding materials could be damaged by constant radiation due to interaction with each other [3][4].

1.2 Genetic algorithm

Genetic algorithm is an natural selection on a computer, it makes biological evolution in a computational model. John H.holland was the first one who establish the biological evolution as a model and developed this method. In the long period, the creature has gradually adapted to the environment during its continued existence of biological process, and it was improved. The base of evolution is the improvement of individual. Each individual has different ability for different living environment. According to Darwin's theory of evolution, those with a strong ability to adapt to environmental change are more viable organisms, have bigger chance to survive, and that creature may have more offsprings. Those with a weak ability to adapt to environmental change are doomed to disappear. This is called "natural selection, survival of the fittest." Through natural selection, species will gradually improving to survive in the living environment, and finally some developed species appear. Following the biological evolution, a GA allows a population which is composed of many individuals to evolve in specified selection rules to a state with best fitness

The basic theories of Genetic algorithms can be divided into four parts

1.2.1 Original population

GA is based on populational optimization algorithms. The process of searching optimized solution starts from one original population. The original population was often generated by a random method. The original population determines the time cost in searching. And experiential data can help to cut searching time, but, it may lead to a factually incorrect result. So this section requires elaborate work.

1.2.2 Construction fitness function

The key point in Genetic algorithms is the construction of a fitness function. Employing this function, we could evaluate the individual "healthy" which determines the chance of this individual to live longer or has descendants. In another words, it determines the individual or solution whether fits our requirement or not.

1.2.3 Selection and evolution

Natural selection in GA is associated with the fitness value. With a higher fitness value, one gets a bigger chance of survival and multiplication, and vice versa. The average fitness value of population may rise, it is the symbol of evolution.

1.2.4 Optimized solution obtained

If the average fitness value rises to a maximum, we may get a preferable individual with the highest fitness value in the population. Admittedly, this is, maybe, not the real best, but compared with the endless time of searching a real what we got is often acceptable.

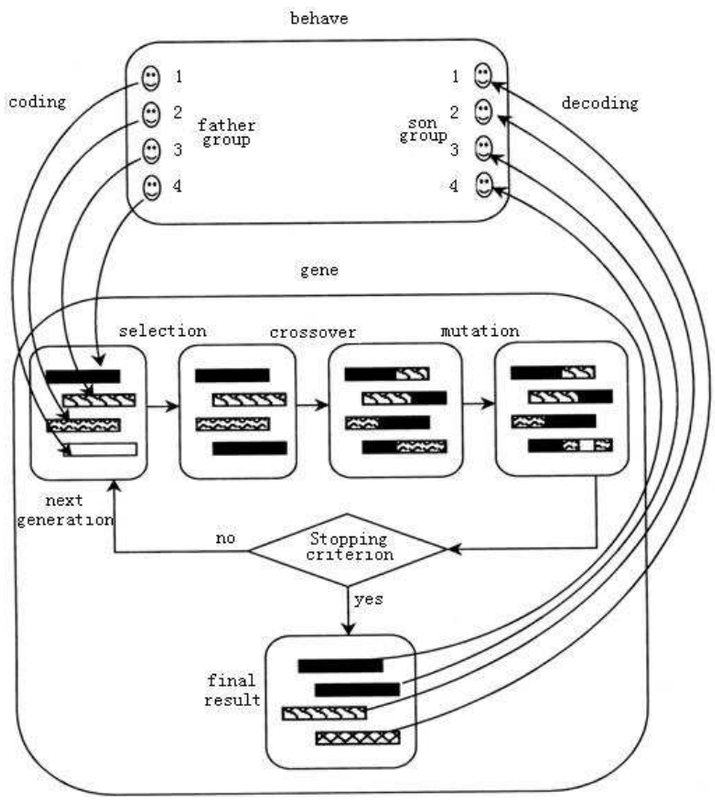

Fig. 3. Encoding Scheme

The following are the key points of GA. The first is population. This population represents one of potential solutions group. Generally speaking, the larger the population size is, the better result we will get. But, it will take more time for calculating. The second is Encoding Scheme (gene representation), Fig.3. Each individual in population is actually the entity with characteristic chromosome. Chromosome is a combination of multiple genes. The combination of genes determines the performance of individual. It requires help from genes to set up the relationship between chromosome and the solution to the optimization problem. That is the encoding of chromosome because of the complexity of encoding. We often employ a easy method, binary encoding, to simulate the gene encoding. The third is Genetic operator, it includes crossover and mutation. It simulates the natural process of reproduction, and it shows the relationship of chromosomes. The fourth is selection tactic. It reveals a natural law of "natural selection, survival of the fittest." in biological evolution.

1.2 GENOCOPII

In our work, GENOCOPII [5], which can prevent us from the trouble of details in Genetic algorithm code, is employed. It is a higher version of GENOCOP which is the acronym of Genetic Algorithm for Numerical Optimization Problem for Constrained Problems. It is a genetic algorithm-based program written in C for constrained and unconstrained optimization.

1.3 MCNP code

The MCNP code [6], an internationally recognized code for analyzing the transport of neutrons and gamma rays by the Monte Carlo method, is developed and maintained by Los Alamos National Laboratory. This code treats transport of neutrons, gamma rays, and secondary gamma rays stemming from neutron interactions. The MCNP code of a higher version can also deal with the transport of electrons, both primary source electrons and secondary electrons created in gamma-ray interactions. The MCNP code has an input file. In our case, there two named inpn and inpp to feed the code with the information calculating

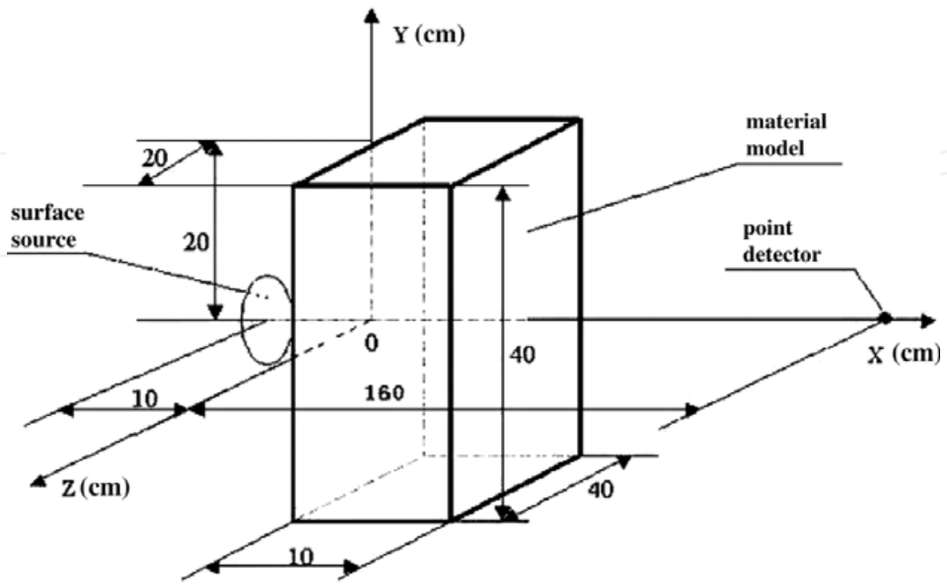

Fig. 4. Schematic diagram

neutrons and gamma rays. Then the calculation finished, the output file with the result is obtained. The figure, Fig 4, is the schematic map of a virtual experiment ran in MCNP code to evaluate the shielding capability of materials.

2. Mathematical modeling in optimal design of shielding material

The optimal design of shielding material focus on the dose equivalent left in the case that neutrons and gamma rays penetrate a specific thickness of the shielding material.
We employed a round surface with fission energy spectra as a radiation source, the dose equivalent corresponding to 2.407 neutrons and 7.77 photons (these are the average number released per fission event [7]) was selected applying the optimized objective function [8][9], this function subjects to certain constraints: equalities, inequalities and domain constraints. They depend on the uniformity of the composite material components, the component range of every element in composite from minimum to maximum, and the density of composite materials:

The Object and Fitness Function:

$$\min f(X) = [f_n(X), f_g(X)]^T \tag{1-1}$$

where:

$f_n(X)$ —total dose equivalent of neutrons and γ-rays with fission energy spectra in one time fission process penetrating a specific thickness of the shielding material, Sv

$f_n(\mathrm{x})$ —contribution of neutrons in dose equivalent, Sv;

$f_g(\mathrm{x})$ —contribution of gamma rays in dose equivalent, Sv;

X — the variable vector, mass components matrix in composite material, $X = \left[x_1, x_2, \ldots, x_p \right]^T$, where x_i （ i =1,2,…,p） is the components material ratio.

The constrains:

$$\sum_{i=1}^{p} x_i = 1 \tag{1-2}$$

$$10/\rho(X) = \sum_{i=1}^{p} \frac{10}{\rho_i} x_i \tag{1-3}$$

$$\rho(X) \in D \tag{1-4}$$

$$L \le X \le U \tag{1-5}$$

where:

x_i —subjects to constraint of normalization

$\rho(X)$ —density function of single component and composite material,

D —vector of the density ranges.;

L , U —components vectors of minimum & maximum respectively

3. Process of optimal design of shielding material

3.1 Optimal design

The Fig.4 shows four steps in the GA optimization design program. These steps can be divided into two parts, the first and last steps belong to GENOCOPII part, and the others are MCNP part. The MCNP code here plays a role like one fitness function evaluating shielding capability of materials. There also lies constrains of materials density, components ratio we focus on in GENOCOPII. Firstly, the raw materials are selected from the present materials (simple elements or compound materials) in the world. The MCNP code is recognized for analyzing the transport of neutrons and gamma rays, but its materials part is not so good. It is next to impossible to simulate the real materials but the virtual one of homogeneous mixture of certain elements. In the process of selecting, the cost and the radiation shielding capability are mainly concerned. Their physical and chemical capability, mechanical and thermal properties are also considered by experience. Secondly, according to a component material ratio assumed originally, each virtual materials density, and all other parameters were edited in the proper MCNP input files: "inpn" and "inpp". After that, MCNP calculates one fission neutron dose equivalent Hn (in output file outpn), one

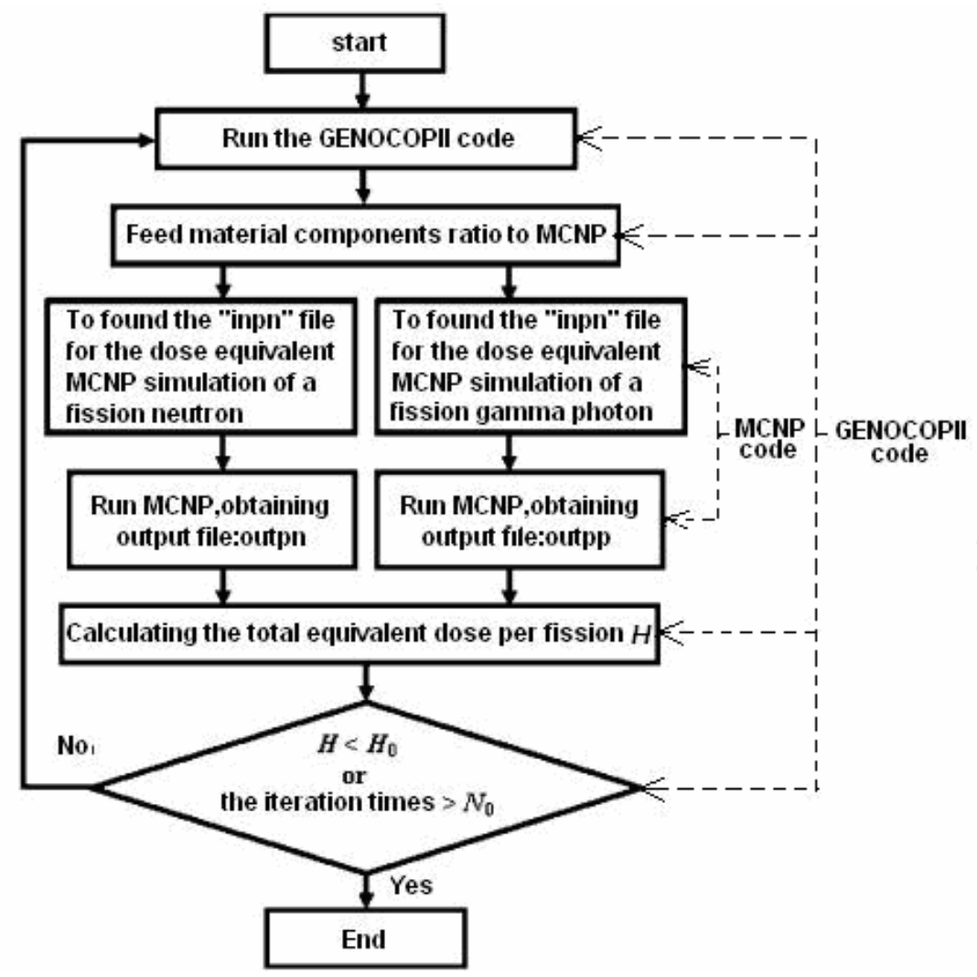

Fig. 5. Optimize procedures

fission photon dose equivalent Hp (in outpp), and the total dose equivalent of the neutrons and -rays per fission. Thirdly, the GA program can transfer the MCNP results at every generation in every count, if so needed. Finally, the object function for optimizing design is a certain function, based on constraint conditions confirmed by some calculations.
The achievement of the final goal, a qualified shielding material, requires an exploratory stage. This indispensable stage sloves some problems, such us, the selection of raw materials, evaluation of components vectors of minimum & maximum respectively, experimental research on manufacturing process, et al.

3.2 Simple cases of optimization design on shielding material

By running the optimal design program, a series of materials optimized ratios have been obtained. They are listed in Table1. Jxa1 and Jxa2 are polyamide composites, Pb6 is anhydride composite, Djy is another composite suited to powder forming with heat isostatic pressing (HIP). Interlayer is also polyamide composite without Fe, W and Pb.

element	H	^{10}B	^{11}B	C	O	Ti	Fe	Gd	W	P	density /g.cm^3
Jxa1	2.226	0.316	0.581	17.88	5.307	0.06	0	1.736	5.013	67.29	3.38
Jax2	2.45	0.078	0.31	18.5	5.31	0.06	0	1.74	12.67	57.73	3.53
Pb6	1.523	0.366	1.466	14.567	5.056	0.379	0	0	14.436	62.186	3.72
Djy	0	0	0	26.28	1.95	0	50.17	12.80	8.80	0	5.7
Interlayer	8.19	0.16	0.64	65.87	18.43	0.93	0	5.78	0	0	1.48

Table 1. Shilding material element contents optimal designed /W%

Components	Name	Formula	Density/ g·cm^{-3}
1	Graphite	C	2.25
2	Carbonization boron	B_4C	2.52
3	Nano TiO_2	TiO_2	0.86
4	Oxidation gadolinium	Gd_2O_3	7.4
5	Iron	Fe	7.86
6	Tungsten carbide	WC	15.5
7	Lead	Pb	11.342

Table 2. The optional shielding materials components under Polyester composite process

The Fig.6 shows the relationship between total dose equivalent and generations of Jxa1.Its obviously that with the population evolution, the value of objective function, that is total dose equivalent, decreases. When the number of generation grows up to 40, the total dose equivalent seems steady. And the individual with best performance having components information is obtained.
Our program works well. Furthermore, according to the interaction mechanism of neutrons and other materials, we develop a multilayer material. The first layer iron is quite effective to slow down the fast neutrons to intermediate neutrons by inelastic scattering. The middle

is the Interlayer, cake, which not only slows down intermediate neutrons to thermal neutrons by elastic scattering on hydrogen (8.19w%) effectively, but also captures thermal and intermediate neutrons by boron-10 (0.16w%) and gadolinium (5.16w%). The last layer, lead, can attenuate the γ -rays and the secondary γ -rays of neutrons. Iron and lead are the common shielding materials for theirs low price and easy machining. But they cannot be used extensively due to the weight and volume limit. Therefore their thickness component ratio is optimized. The Cakes shielding capabilities were simulated.Fig.6.

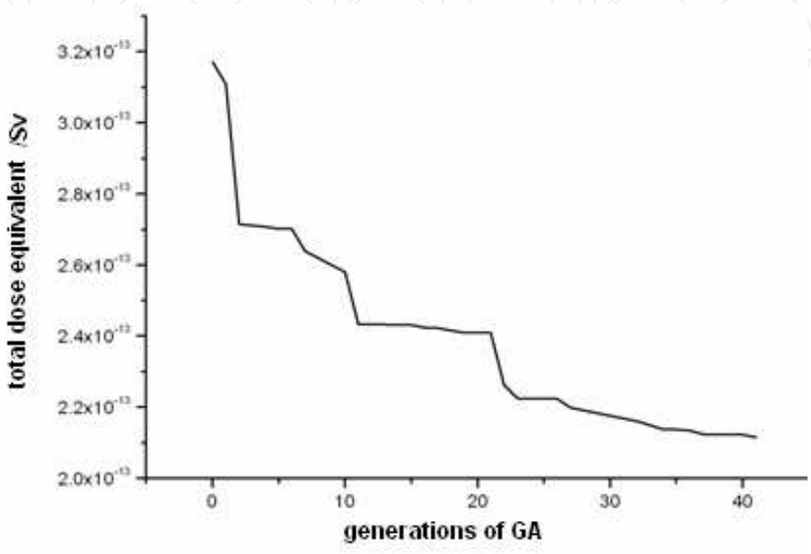

Fig. 6. Total dose equivalent

However, the MCNP code is of low efficiency due to Monte Carlo method. It may take a long time to combine the MCNP code with genetic algorithm for calculating, so we hope MCNP code may give way to some deterministic method. The method of fission neutrons removal cross sections to calculate radiation shielding can be found in some references [10]-[12]. But there lie two problems that have not been solved thoroughly: attenuation of low energy neutrons (thermal and epithermal) and inelastic scattering of fast neutrons.

Further studies may focus on developing a comprehensive optimization design which not only considering the shielding performance but also stability of material in irradiation and other requirements. One promising method is using the multi-scale modeling to predict life span of certain material [13].

4. Trial-producing the composite materials

4.1 The development of the polymer-based composites materials technology manufacture craft

The solid of the resin composites refers to the curing reaction of polymer materials, namely resin cross linking by linear molecular structure change into three-dimensional reticular molecular structure. With the difference of the resin curing temperature and the length time, its solid degree is different. So, having researched the process of the resin curing, we can obtain the relationship between the solid time of the resin curing and temperature. Then employing the variable time and temperature we could change the mechanics and thermal properties. In this paper we used the DSC to analysis solid degree [14].

4.1.1 Resin material

Lots of thermosetting and thermoplastics can be used as composite resin. From the present situation, the commonly used of thermosetting resins are: unsaturated polyester, ethylene polyester, epoxy, phenol, BMI and polyimide matrix, table 2, The common thermoplastic resin: polypropylene (PP), polycarbonate (PC), Nylon (Nylon), PEEK (PEEK), polyether (PES), etc. In the aspect of bearing temperature, heat-resistant performance is superior to thermoplastic resin.

Because the raw materials of the bisphenol A (2) phenol is easily obtain, and it is the cheapest, so the output is largest, about 85% of the total output of epoxy resin[15], people also referred to it as general epoxy resin. The temperature in this research is 273-573K, the bisphenol-A type of epoxy resin can meet the requirement. In addition, it has the advantage of curing, price, molding, etc, so we used the bisphenol A type of epoxy resin type which can meet the requirement, adding to the advantage of curing, price, molding, etc, so we used the bisphenol A type of epoxy resin composite material.

1. the structure of the bisphenol A type of epoxyresin[16]

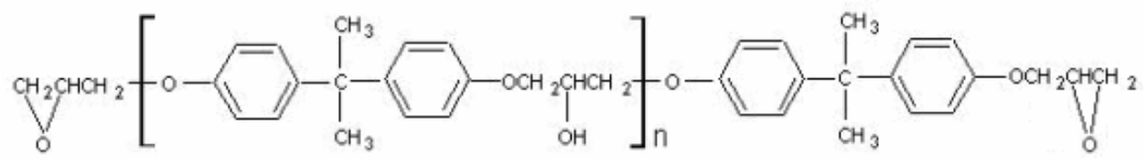

2. epoxy resin curing reaction

Through the analysis of the essential resin curing materials, this paper has selected the materials as belows: E - 51 bisphenol A, PMDA, MA, epoxy propane butyl ether and TiO_2 as the part of resin, the specific materials reaction process as follow [17]:

1. first the the epoxy resin reacts with anhydride then producing carboxylic acid which containing ester chain:

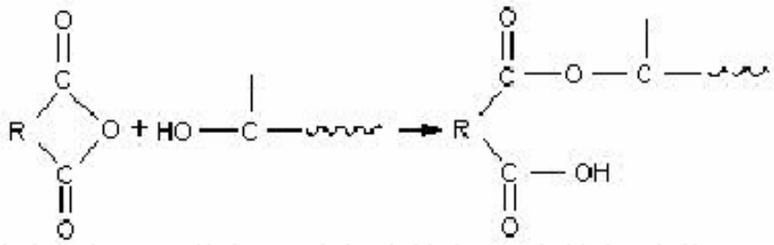

2. Carboxylic acid and epoxy resin epoxy open cycle-addition reactions generating para-ammonium hydroxyl:

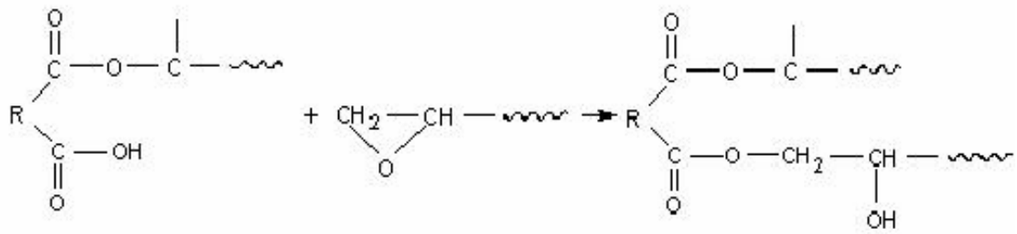

3. the produced hydroxyl react with another acid anhydride (the response equation is the same as (1), simultaneously with the reaction (4))

4. the produced para-hydroxyl again react with another epoxy

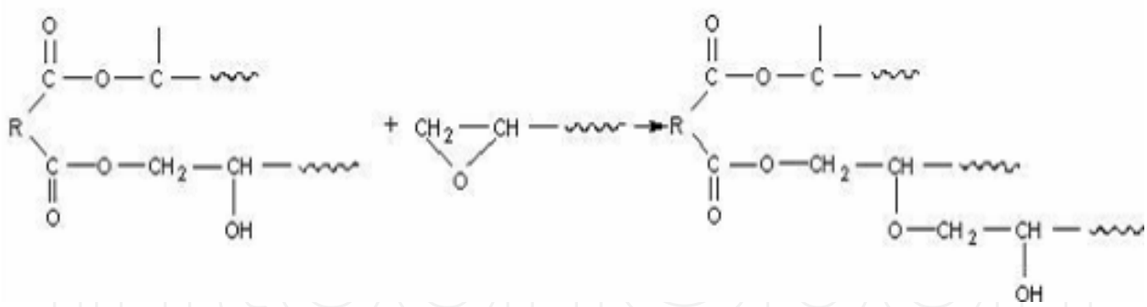

4.1.2 The experiment of differential scanning calorimeter (DSC)

The DSC (Q1000 V9.0 Build 275) used in this experiment is produced in the company TA of American, as shown in figure.7. The temperature range: 180-998K, the experiment using nitrogen gas conduct the heat, the flow speed is 50.0 ml/min, accuracy: ± 0.5K, the sensitivity: 0.2 0.2μW, error range: 1%.

Fig. 7. Q1000 Build 275 DSC instrument

1. Experimental material.

The raw materials used in this experiment as shown in table 3.

component
E-51 bisphenol A
PMDA
MA
Epoxypropane butyl ether
Pb
Fe
Rutile nanometer TiO_2
Total mass

Table 3. Raw materials for the experiment

2. the experiment scheme[18-20].
(1) put the mixed samples into DSC pool, choose the warming speed :2.5K/min, 5 K/min, 10 K/min and 20 K/min, and then scanning from 283K to 572K, obtain the trends warming curves as ,as shown in figure. 8.
(2) According to the dynamic scanning exothermic curve, The beginning, peak and the end temperature of solidification with constant surrounding temperature can be extrapolated.
(3) According to the initial curing temperature we selected four samples temperatures, we solidified the sample1, sample2, sample 3, samples4 and sample 5 separately at these constant temperatures.
(4) After the constant temperature solidification, cool the samples at the rate of 10 K/min to surrounding temperature. And then operating the DSC at the same rate. Finally, we obtain the reaction surplus heat and the vitrification temperature.

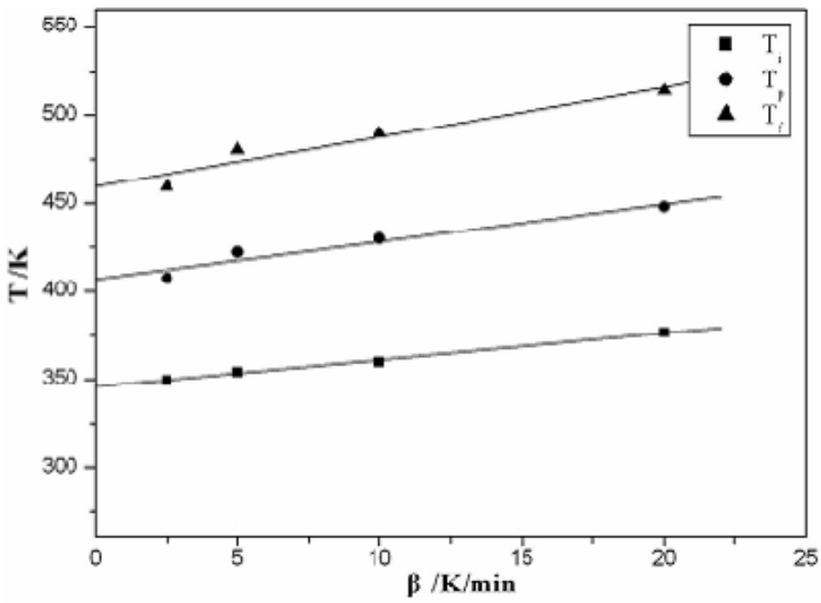

Fig. 8. The characteristicof sample 3 at difference sweepspeed

4.1.3 The thermal analysis results and discussion

1. The vitrification temperature

The vitrification temperature is in agreement with curing temperature, but high curing temperature will reduce curing degree, see figure.9. While the vitrification temperature is related with nanometer TiO2 Accounts for 3% of bisphenol A, the vitrification temperature reaches extreme, as shown in figure.10.

Through the nonisothermal curing DSC scans, it found that the TiO_2 can reduce the resin's curing temperature and promote the release heat of solidify effectively, and then the curing product's vitrification temperature also have certain effect, at the same temperature, when TiO_2 take up 3% of bisphenol A , the vitrification temperature is the highest one.

In a certain temperature range, the increase of isothermal curing temperature can increase the vitrification temperature of the curing product.

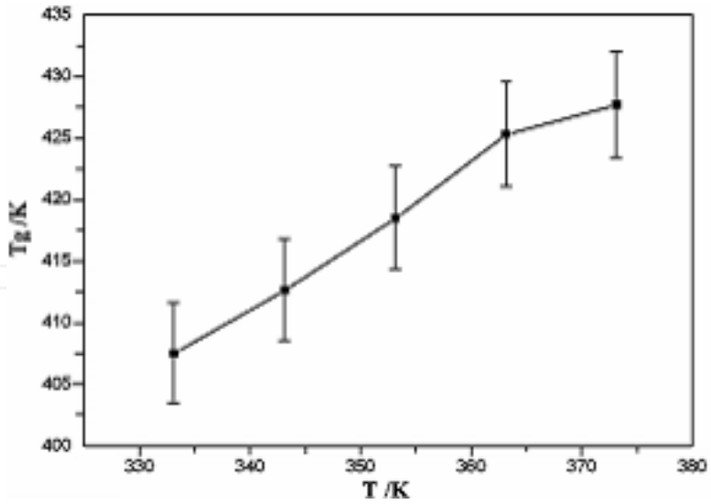

Fig. 9. The isothermal curing temperature determines the vitrification temperature

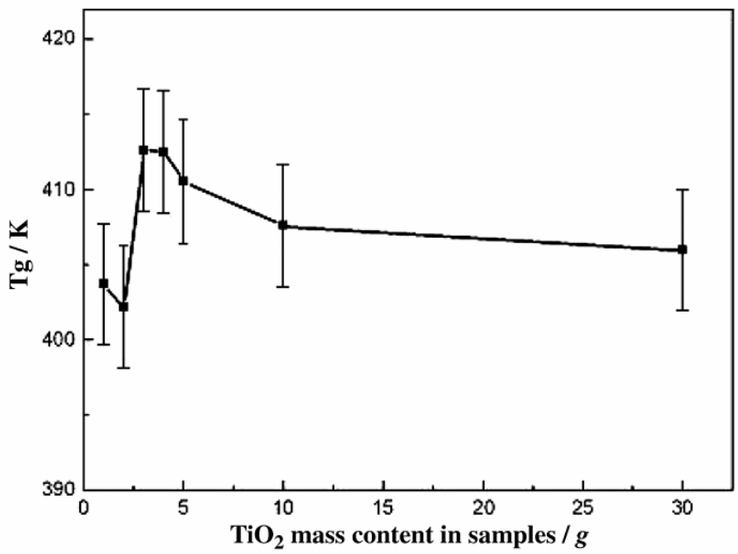

Fig. 10. The relationship between vitrification temperature and TiO2 content at 343K

4.2 The trial-producing process

According to trial-manufactures of composite materials and the characteristic of the shielding composites, the preparation process can be divided into four stages:

1. Preparation

(1) dube the silicon oil inside the surface of material molding, placed it around 1 day, standby, as shown in Fig.11.

(2) According to the proportion weighting PMDA and MA, make it into powder and blend equality, put it into the bottle, then placed the bottle into the heater heating until it completely melt.

(3) According to the proportion weighing iron powder (Fe), lead oxide (Pb), carbonation boron (B_4C), tungsten (WC), graphite (C), titanium dioxide (TiO_2 and trioxide gadolinium (Gd_2O_3) and propylene oxide butyl ether, etc.

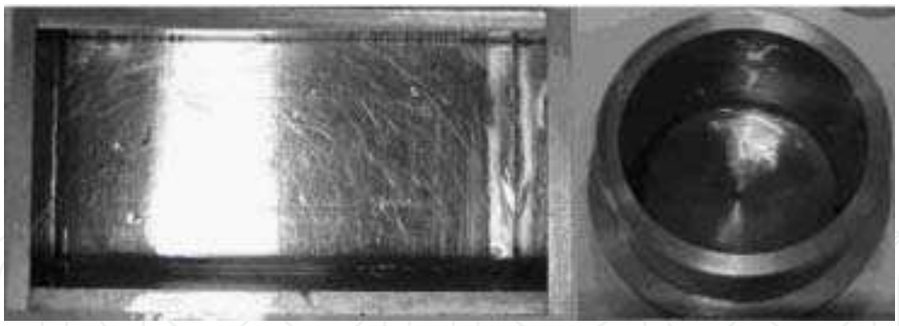

Fig. 11. Materials moulds

(4) Put bisphenol A on electric stove heating, melting weighing.
(5) Blending the bisphenol A PMDA with MA and stir well, then pour epoxy propane butyl ephedrine and TiO_2, stir well.
(6) Put the enhanced mutually particle into the mixture solution.
2. The former dispose of material solidified
(1) Put the mixed well materials into the blender, stir well with different rotate speed
(2) Put the mixed well materials into the vacuum air exhaust containers, exhausting until the vacuum degree no longer change.
(3) Repeat a and b two or three times then pouring mold, put the forming materials into containers, again exhausting several times.

Fig. 12. Vacuum blender

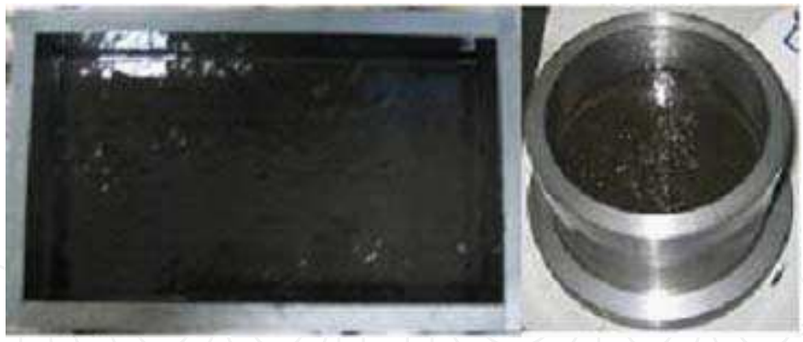

Fig. 13. The polymer poured into the mold

3. Materials solidify

(1) Put the forming container into the designated temperature preheating constant temperature box, curing at constant temperature.

(2) The first stage of curing is over, making the constant temperature box rapid-heating until the curing temperature, and then curing.

Fig. 14. The constant temperature box

4. Mold unloading

Get out the cured materials, the mold unloading sample is shown in Fig.15.

Fig. 15. The mold unloading sample

4.3 The samples of materials

According to the result of the optimization design material composition and the established industrial art technological process, it design a series of new polymer radiation shielding materials, polyamide as the curing agent of samples Jxa1 (Fig.16) and Jxa2 (Fig.17), mixed anhydride as curing agent of sample Pb6 (Fig.18), and polyamide as curing agent and has no metal particles of inorganic polyester with filling samples Interlayer (Fig.19) without Gd_2O_3.

Fig. 16. xa1 samples (cylindrical)

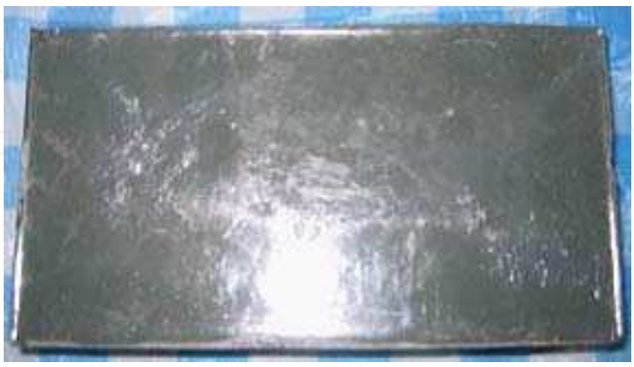

Fig. 17. Jxa2 samples

Before curing material the air exhaust is very important, because it dose good to low material's internal porosity rate, thus improving the uniformity of the internal structure and the mechanical properties of materials.

Fig. 18. Pb6 samples

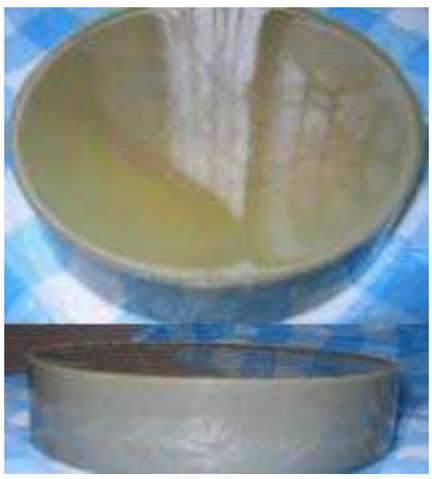

Fig. 19. Interlayer

Fig. 20. Djy samples without the hydro form formed

5. The test of shielding material performance

5.1 The neutron shielding assessment experiment device

5.1.1 The general situation of serial electrostatic accelerator neutron source system

1. the mainly configuration

5SDH-2 serial electrostatic accelerator neutron source system (shown in Fig.21).

(1) Ion source

SNICSII type sputtering ion source.

(2) Injection

A double-slit lens, x-y roll cone, vacuum pump, and Michael Faraday deflection magnets, single lens.

(3) Accelerator form

Metal tube, two ceramic acceleration transmission chains, peel, the corona pin and high voltage undammed controller, voltmeter, rotation system, vacuum pump and control console.

(4) The focus on magnetic analysis system

Double the lens, switch magnets, Y guide.

(5) Beam pipeline

Two 1.5 m long beam pipeline.

(6) Recycling systems

SF_6 gas recovery system.

Fig. 21. The serial electrostatic accelerator system

2. Other supporting system

(1) The neutron monitoring system

BF_3 long used for neutron probe, more, The beam from a different direction deviation from pipeline at different distances from the target to hit the neutron beams.

(2) Positioning system

Contains the sideway, optical centre aligning, and TV monitoring system.

(3) Data acquisition

NIM standard system.

(4) Main technical indices

Neutron emission strength: 10^9n/pulse,

d - D reaction: can produced in the 3-7MeV points neutrons,

d -T reaction: can produce under 3MeV point's neutrons.

5.2 Shielding material evaluation experiment

5.2.1 The layout of evaluation experiment

In the use of ^{252}Cf spontaneous fission neutron source shielding materials of samples of neutron shielding effect evaluation experiments, source, detector and neutron probe general layout as shown in Fig.22. The dotted line in the red circle diagram in front of detector have a homemade container, above it is a polyethylene cylinder. So, it can ensure that the backward play source efficient and accurate. Ensure radiation safety, what the picture have done also through the neutron shadow cone and alignment holes to keep out. Likewise, when shielding material sample absorbing neutrons, unload the neutron shadow cone, and put the thickness of shielding materials which to be examined on the neutron beams on channel, the subsequent transmission neutron probe is needed before receiving throughout the sample.

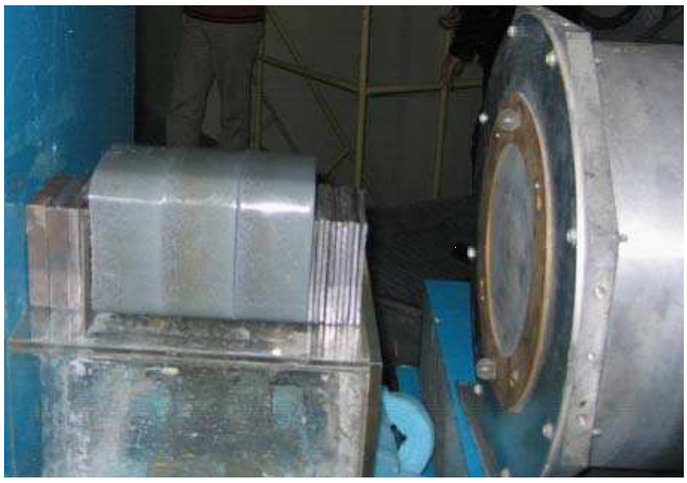

Fig. 22. The measurement of Sample neutrons shielding materials absorption

5.2.2 The experiment principle

Set the neutron various through the thickness measurement's flux data is $\phi_i i = 1,2,3$, A sample tested before and once measured this bottom flux measurement and neutron flux material , take two measurement flux average ϕ_b and ϕ_0 , The through rate of the samples of neutron is $i = 1,2,3$ By the type,

$$T_i = \frac{\phi_i - \phi_b}{\phi_0 - \phi_b} \tag{1-7}$$

5.2.3 The experimental results

To develop the jxa1, jxa2, pb6, Cake1, Cake2, Cake3 and multilayer compound shield Fe - CH_2 - Pb, All of which had experiment examined.

For example ,we only use polyester sandwich materials Cake1's (with iron and lead, equivalent density, 4.554g·cm^{-3}) experimental results of assessment of the data processing to analyzed and discussed and compare with the numerical simulation results and multilayer composite shielding experimental results numerical simulation results.

Composite multi-layer Fe shield - CH_2- Pb`s Data can be gain acceding to (1-7), every weaken ratio's indeterminacy lie on $\phi_i$ , $\phi_b$ , $\phi_0$ `s indeterminacy and themselves .

$$\frac{\Delta T}{T} = \pm\left[\frac{(\Delta\phi_i)^2 + (\Delta\phi_i)^2}{(\phi_i - \phi_b)^2} + \frac{(\Delta\phi_0)^2 + (\Delta\phi_b)^2}{(\phi_0 - \phi_b)^2}\right]^{\frac{1}{2}} \tag{1-8}$$

Due to ϕ_b and ϕ_0 is difference, in the experiment, the difference is 10 times, so the type can be simplified as follow

$$\frac{\Delta T_i}{T_i} \approx \pm\frac{[(\Delta\phi_i)^2 + (\phi_b)^2]^{\frac{1}{2}}}{\phi_i - \phi_b} \tag{1-9}$$

So, we can press get the uncertain result from (1-8) which gives the weaken ratio.

By the type of (1-8), we could see that with the more thickness of the shielding materials, ϕ_i is gradually approach ϕ_b , Transmittance T_i 's relative uncertain fierce raise, the behind data points can be even discarded.

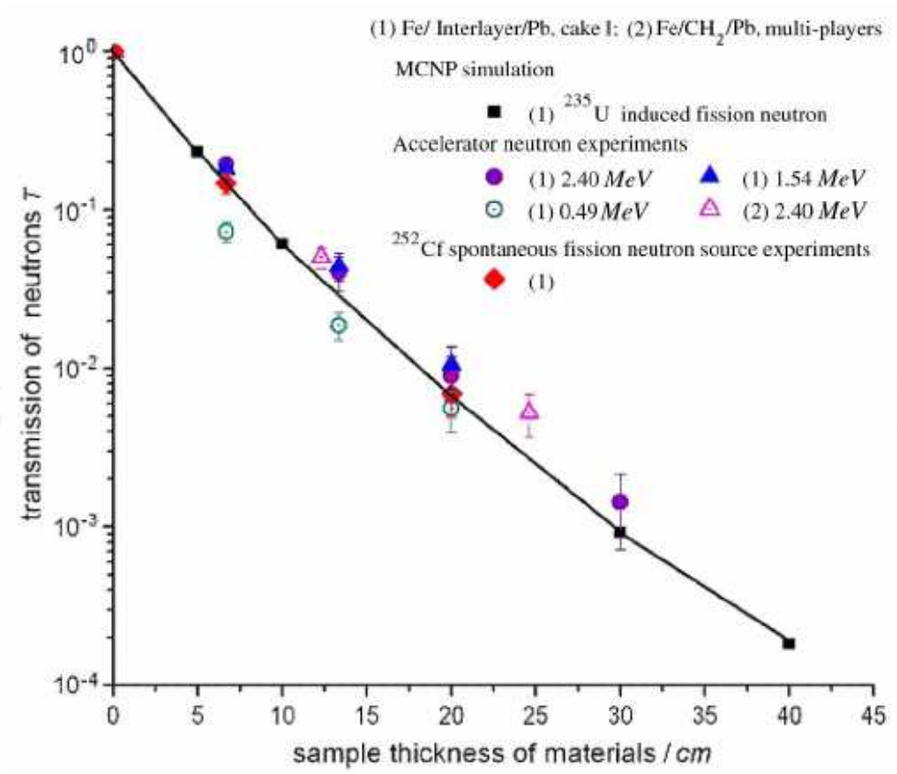

Fig. 23. Experimental test on neutron shielding performance of Cake1 and comparison to Fe/CH_2/Pb multi-layers

Fig.21 Cake1 gives the situation of, 2.4 MeV (purple, circular) 1.54 MeV (blue, triangles), 0.49 MeV (turquoise, circle), three accelerator neutrons` cross rate. The picture also gives experiment date (red, lozenge)of the ^{252}Cf fission spectrum source's through rate, and also gives the neutron penetration curve (black, square)of the MCNP's complete theoretical simulation of neutron spectrum (and the difference with ^{252}Cf fission spectrum are tiny). We found that the experimental through rate data of the neutron spectra neutron source was fall on the theory simulation curve, this show that within the thickness the neutron penetrate shielding materials simulate theory is correct, the simulation of materials from the design and manufacturing process through examination results are success.

As show in Fig.23, multilayer composite shielding body sample gives the date of two thickness at the energy points of 2.40 MeV (purple, upward triangle) ,The effect of neutron shielding is worse than the polyester sandwich material at the same conditions (with iron and lead).

As shielding materials is more and more thickness, it is obvious that the phenomenon of the through rate `s uncertain is fierce raise.

5.3 The experiment principle

As shown in Fig.22, it is a device to check the effect of the shielding materials, NaI (Tl) energy spectrum detector. The left two peaks in Fig.23 namely are the γ-rays of $^{60}C_O$ two all-powerful peaks.

Set the various thickness measurement of rays all-around peak counts word address range is, $I_i, i = 1,2,3$, Before and behind the test, we test the sample without the material and counting , take an average of two counts as I_0 , Then the various thickness of the sample`s weakened ratio is $T, i = 1,2,3$, the calculate formula as follow.

$$T_i = \frac{I_i}{I_0} \tag{1-10}$$

The biggest advantage is that the counting time can be control by people, increasing the count time can reduce the uncertainty of experimental data. But when the source of is low activity, the work efficiency is low. And when we choice higher activity source, proper handle radiation safety issues, it will make the efficiency greatly improved.

Fig. 24. The experiment of the device of radiation absorb

Fig. 25. The γ-rays energy spectrum of $^{60}C_O$ tested by NaI(Tl) device

The Measurement data isn't more, the focuses is to choice the function of the sample shielding material, then it could tell us the optimum design method and the development process whether meeting the requirements or not. The Material sample chooses Cake1 and multilayer composite shield Fe - CH2 - Pb (6/3/1).

density / g·cm^{-3}	thickness / cm	totalize count	completely area	Weaken ratio	The simulate of Co	The simulate of fission spectrum
Cake 1 （4.554）	0	234550	128205	1	1	1
	6.67	54689	23255	0.1814	0.1841	0.2418
	10	27430	9616	0.0750	0.0790	0.1250
	16.67	8150	1250	0.0098	0.0148	0.0357
	20	5335	284	0.0022	0.0064	0.0194
multilayer （6.126）	0	234550	128205	1		
	6.67	43518	12828	0.1001		
	13.34	10143	832	0.0065		
	0	72839	31151	1		
Jxa1	9.47	16662	5822	0.1869		
Pb6	9.35	14356	5126	0.1646		
Jxa2	0	29718	16435	1		
	4.6	15661	7795	2.1000		

Table 3. The test result of two kind of materials $^{60}C_O$ radiation's weaken ratio

The measuring results see Table 3. The weaken ratio in the table counting according to the formula (1-10).

The uncertain of the weakened of the ratio`s depends on I_i, I_0 and itself,

$$\frac{\Delta T_i}{T_i} = \pm\left[\left(\frac{\Delta I_i}{I_i}\right)^2 + \left(\frac{\Delta I_0}{I_0}\right)^2\right]^{\frac{1}{2}} \tag{1-11}$$

So it can estimated weaken ratio acceding to (1-11). In the experiments it observed the fundus, we discover that the rang of fundus' peak is so tiny, then it could be negligibled, this is the advantage to use the devise to test the weaken ratio.

Fig.20 presents the icon of table 1-4. From the picture we could see that the sample of Cake1 shielding the$^{60}C_O$ (red and black) is better than the fission spectrum rays (blue), and with the thickness increase it will be better and better. Then we only see $^{60}C_O$ γ radiation, the theory simulate date (red) is higher than the experimental date (black), its reason is that the accumulation effect is action.

Theory simulation need materials large enough ,the cross-section ought to 40*cm**40cm, but experiments Cake1 diameter only 15cm, the Fig.25 is better effect that only part of the multiple scattering rays in the experiments Cake1 sample get point detector (the sensitive area is lesser). So Fig.26 gives a dotted line. The dotted line reflects the situation that the accumulation effect is corrected similar to date imitate. Then, we could draw the conclusion that the numerical simulation and experimental results are basically the same.

Get such conclusion no double illustrates that the design of the sample to shielding the □ray as we expect , and the materials design craft reach the standard , therefore the performance of the sample shielding ray is reliable.

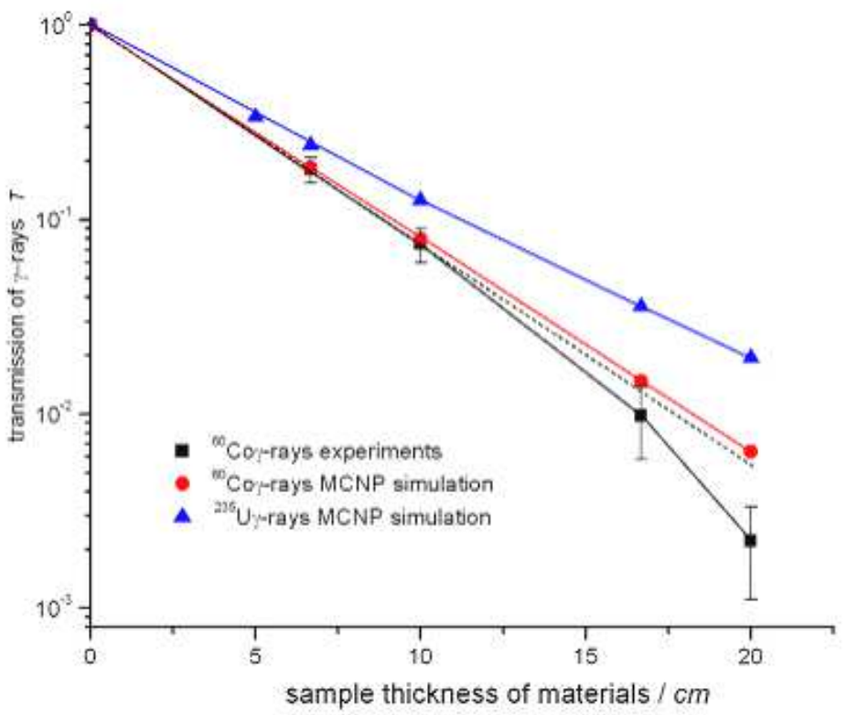

Fig. 26. The compare of the result of the Cake1sample neutron weaken ratio experiment and the result of date simulate

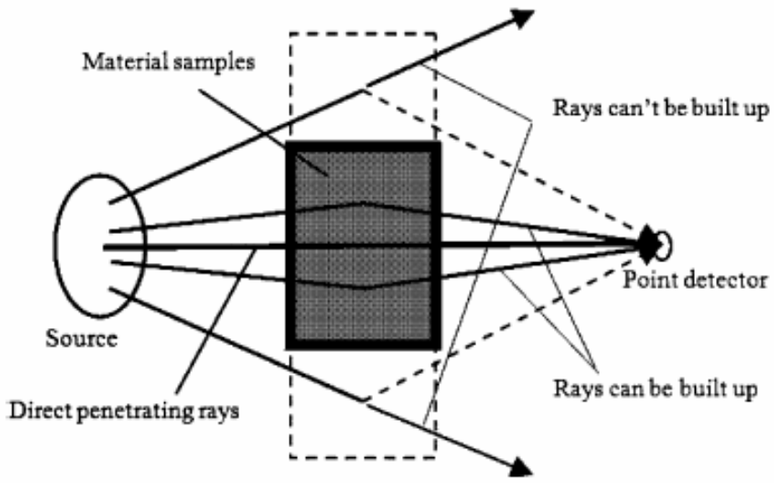

Fig. 27. The part accumulate effect of the γ-ray pierce the limited scale materials in experiment

5.4 The check experiment of the sample's machinery performance

The experiment mainly determined the draw intensity of the sample Jxa1 (including tensile rate) as shown in figure.25, the experiment test the compress stress of Jxa1, Interlayer and Pb6 as shown in figure.26, it list the comparison of the result of the shielding materials machinery performance and PB202 products.

a) b)

Fig. 28. The determine experiment of the samples Jxa1(including tensile rate)
a) The draw experiment of Jxa1 b) the breaked experiment sample of Jxa1

From the table1-6, we may could see:
(1) the draw strength of the sample Jxa1 is twice more than PB202 , therefore can used at the more acuity environment.
(2) From the result show when the compression stress is 50%, the two material,
Jxa 1, Interlayer, could keep relative integrality after it endure great pressure.
This is great advantage when it mentioned to the situation to remain the integrality of the shielding materials. The solidify agent of Pb6 is mixed acid anhydride, the trial-producing

craft is complex, the combine uniformity is relatively poor, add to the precipitation phenomenon the heavy metal material s itself, the layering phenomenon still more obvious, therefore it exists scatter in the anti-compress experiment result. The behind two dates listed in table 3 is anti-compress strength.

(3) because the materials is polymer, the softening point temperature of it is large more than PB202 which containing large Numbers of polyethylene much, then the obtained materials in study will have more extensive application. The date listed in the table is the solidify temperature at which the materials has solidified, the softening point naturally higher than after solidify temperature.

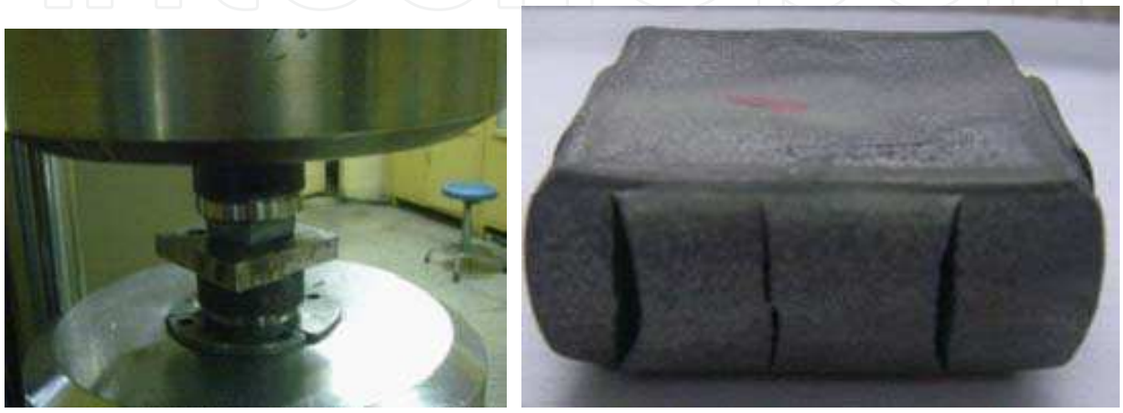

a) b)

Fig. 29. The experiment to determined the compressing stress of the shielding materials' sample. a) The compressing stress test of the sample, b) The compressing stress sample of Jxa1 when it was compressed to 50%

The code name of materials	density /10^{-3} kg□m^{-3}	the soften point /℃	the draw srength /MPa	The draw rate* %	Stress at the compress of 50% /MPa
PB202[9]	3.42	99	12.63 +	——	——
Interlayer	1.48	>140	——	——	152.47
Jxa1	3.43	>140	25.82	8.6	148.07
Pb6	3.72	>160	——	——	133.09，148.96，193.05

*:refers to Chinese national standard GB/T6344-1996; #:refers to Chinese national standard GB6669-2001; +: literature[9] isn't say the experimental standard

Table 4. The compare of the shielding materials` machinery performance and the PB202 products

5.5 The experiment of the shielding materials sample's metallographic

5.5.1 The process of prepare the sample

(1) Sampling

Get a 10×10×20 cuboid from trial material, and then make a cylinder which diameter is 10mm.

(2) Embedded

Make the prepared cylinder stick to the prepared rob tool, use it after solidify.

(3) Grind

Firstly, Use the 280 # sand paper polished the burnishing surface according the requirement again and again, then repeat the process with 4000 #, 800#, 1000# unlit the surface of the sample is smooth.

(4) Polishing

Put the rubbed sample on the polish machine to polish, until the surface smooth and have mirror face effect.

The metallographic experiment samples prepare for the shielding materials sample as shown in figure 27, there have Pb6, Interlayer and Jxa1 three kind of sample, each parallelism the picture (a) , (b) and (c).

a) b) c)

Fig. 30. The metallographic experiment samples prepare for the shilding materials sample a) Pb6, b) Interlayer, c) Jxa1

5.5.2 The experimental observation and analysis

Take a picture and observe the prepared of three kinds of metallographic experiment samples, and every corresponding metallographic picture as shown in Fig.31.

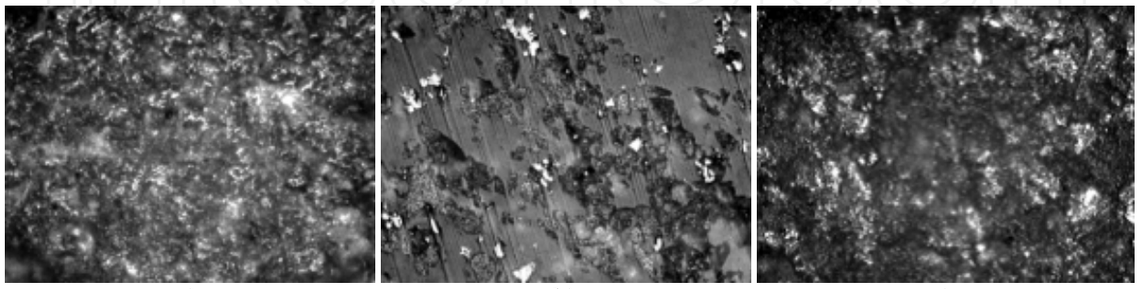

a) b) c)

Fig. 31. The picture of the shilding materials sample in metallographic experiment（magnify multiple: 400), a) Pb6; b) Interlayer; c)Jxa1

From the picture (a), the materials of Pb6 is a mixed acid anhydride, the metal particle combine with the polymer relative asymmetry, In the picture (b), the sample of the polyester of filling use the poly-amine as the solidify agent ,and only have the inorganic metal particle Gd_2O_3 , the B_4C, Gd_2O_3 powered disperse equality in the polymer, from the picture (c), Jxa1 use poly-amine as the solidify agent and add the inorganic power of W, Pb, because it emphasis the problem of precipitation, so the metal particles in polymer dispersion is well-distributed. Generally speaking, except Pb6, when the inorganic metal particle blend with the poly-amine as the solidify agent in material sample (below 200). This particle of inorganic metal powder is enough to develop nuclear shielding materials, the result of the radiation shielding experiments have proved this.

6. Discussion

In GA optimal design and shielding experiments, the selected material geometry model and experimental material samples were just slabs. If cylindrical and spherical geometry model and relative material samples were selected, actual shielding performance could be obtained. In other words, the shielding performance of the materials is better in applications than that in experiments because actual shields mostly have cylindrical or spherical geometry structure.

Due to lower intensities of radiation sources, the material samples are all too thin to test shielding effects perfectly in deep penetration situations in our experiments. The heat and radiation resistance of materials should be studied quantitatively in experiments. Therefore the related experiments should be carried out in the near future.

For the heavy metal powders, such as Fe, Pb and W, mixing with polymer, several precipitation phenomena appeared in the forming process when the mixture consists of high component of polymer, for example, more than 30%. In our study, the efforts to manufacture a new kind of special gradient material (SGM) by virtue of the precipitation phenomena are still under way. A permanent magnet is used to attract Fe powders from the polymer mixture, thus Pb and W powders remain precipitated in the mixture. Then the SGM with “middle heavy-light-heavy” density distribution could be produced. This kind of material is very suitable for the nuclear radiation shielding material.

Because Fe, Pb and W are separated completely to be independent parts of shield, the Cakes are the extreme product of the SGM. Furthermore, because Fe, Pb and W are ordinary materials, the production of Cakes could focus on just the Interlayer.

Fusion neutrons and -rays mixed radiation shielding material could be designed applying our GA optimal design method. It could design not only the shielding material component but also the thickness ratio of shield based on the interlayer products.

The tanks for nuclear fission waste and isotope transportation could be made adopting our interlayer forming technique partially.

7. Applications

The collimators in nuclear radiation measurement system were designed using the cakes to obtain favorable collimated beams requested by experimental physical scientists.

The trial production of the thick pinhole for fusion neutron penumbra imaging has been carried out according to the manufacturing process of shielding material[21][22].

8. Conclusions

The method to optimize in lightweight, compactness and high temperature sustaining for the neutrons and γ-rays mixed field shielding materials was established by genetic algorithms combined with the MCNP code. Several trial-manufacture samples were produced using the related manufacture technology.
Shielding tests of samples verified that the correctness of optimal design method and reliability of the manufacturing process. The results of research can be wide applied to the practices of nuclear science and technology.

9. Acknowledgments

The authors would like to thank Zhiqiang Wang at the Metrology Department of the China Institute of Atomic Energy (CIAE), who provided accelerator and neutron dose monitoring. The authors also acknowledge valuable discussions with Professor Mingguang Zheng at the Shanghai Institute of Nuclear Power Engineering, and Professor Yuangang Duan at the Chengdu Nuclear Power Institute of China.

10. References

[1] T. S. Gates and J. A. Hinkley, Computational Materials: Modeling and Simulation of Nanostructure Materials and Systems NASA/TM- 2003-212163, Mar. 2003, pp. 1–17.
[2] J. W. Wilson, F. A. Cucinotta, M. H. Kim, and W. Schimmerling, Optimized shielding for space radiation protection, *Phys. Med.*, vol. 17 (Suppl. 1), pp. 67–71, 2001
[3] National Council on Radiation Protection, Guidance on Radiation Received in Space Activities, *NCRP Rep.* No.98, Jul. 31, 1989, pp. 1–21.
[4] P. A. Lessing, Development of 'DUCRETE' INEL-94/0029, March 1995, pp. 1–16.
[5] Michalewicz Z, Janikow C. GENOCOP: A Genetic Algorithm for Numerical Optimization Problem with Linear Constrains[J]. *Communications of the ACM*, 1992:175-201.
[6]Briesmeister JF. MCNP : A General Monte Carlo N-Particle Transport Code , Version 4A: LANL Report LA2126252M . New Mexico : Los Alamos National Laboratory , 1993.
[7] N. M. Schaeffer, Ed., Reactor Shielding for Nuclear Engineers, TID-25952, *U.S. Atomic Energy Commission Office of Information Services*, Jan. 1973.
[8] H. Hu et al. Optimized design of shielding materials for nuclear radiation, (in Chinese) *Atom. Ener. Sci. Technol.*, vol. 39, no. 4, pp.363–366, Jul. 2005.
[9] Huasi Hu, et al. Study on Composite Material for Shielding Mixed Neutron and γ-Rays. *IEEE Transactions on Nuclear Science*, ISSN: 0018-9499, 2008, 55(4):2376-2384.
[10] R. D. Albert and T. A.Welton, A Simplified Theory of Neutron Attenuation and Its Application to Reactor Shield Design, Westinghouse Electric Corp., Atomic Power Division, Pittsburgh, PA, WAPD-15, Nov.1950
[11] G. T. Chapman and C. L. Storrs, Effective Neutron Removal Cross-Sections for Shielding, Oak Ridge National Laboratory, Oak Ridge, TN, ORNL-1843 (AECD-3978), Sep. 1955.
[12] A. W. Casper, Modified Fast Neutron Attenuation Functions, General Electric Corp., Atomic Products Div., Cincinnati, OH, XDC-60-2-76,Feb. 1960.

[13] G. R. Odette, B. D. Wirth. Radiation Effects in Fission and Fusion Reactors[R]. *Handbook of materials Modeling*, 999-1037.

[14] Wu Shizhen, Kang Zhuang, Wu Xiaoqing.Using differential scanning calorimetry (DSC) to research the curing system dynamics of TDE - 85/7 # anhydride. *Tianjin polytechnic university journals*. 2005, 24(6): 30-33.

[15] Mi Ae Choi, Mi Hye Lee, Jaeeon Chang, Seung Jong Lee. Three-Dimensional Simulations of the Curing Step in the Resin Transfer Molding Process, *Polymer Composites*, 1999, 4:543-552.

[16] Liu Xiangxuan. The effect of the Composite nanometer TiO_2 to the performance of epoxy resin anhydride(in Chinese). *Insulation communication*.

[17] Wang Dezhong. The production and application epoxy resin (in Chinese). Beijing: Chemical industry press.

[18]Wang Xiaojie, Xie QunHui, zhang wei. The curing study of epoxy resin matrix(in Chinese). *FRP/composite materials*. 2001, 2:1-3.

[19] Chen Xiang, YuanJian, YuLin. Bisphenol A linear phenolic resin curing epoxy resin(in Chinese). *Thermosetting resin*. 2001, 2:1-4.

[20] Shi Zixing. The Synthesis and characterization as well as curing behavior research of Polysulfone polysulfone resin/*Montmorillonite hybrid materials*(in Chinese).

[21] Wu Yuelei, Huasi Hu, et al. The Nature of Single Round Hole Neutron Penumbral Imaging. *Fusion Science and Technology* (FS&T), ISSN: 1536-1055, 2010, 57(3):292-297, American Nuclear Society.

[22] Wu Yuelei, Huasi Hu, et al. obtaining point spread function of penumbral encoding aperture with "expectation maximization" algorithm based on matched source-image pair experiment. *Review of Scientific Instruments* (RSI), 2010, 81(5): 053502-053502-7, 0034-6748.

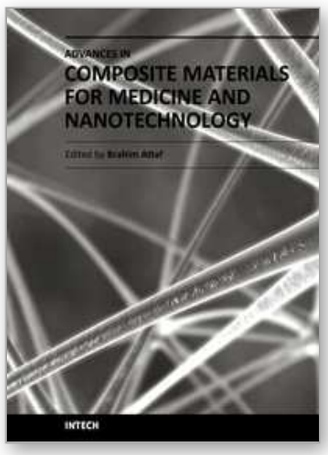

Advances in Composite Materials for Medicine and Nanotechnology

Edited by Dr. Brahim Attaf

ISBN 978-953-307-235-7
Hard cover, 648 pages
Publisher InTech
Published online 01, April, 2011
Published in print edition April, 2011

Due to their good mechanical characteristics in terms of stiffness and strength coupled with mass-saving advantage and other attractive physico-chemical properties, composite materials are successfully used in medicine and nanotechnology fields. To this end, the chapters composing the book have been divided into the following sections: medicine, dental and pharmaceutical applications; nanocomposites for energy efficiency; characterization and fabrication, all of which provide an invaluable overview of this fascinating subject area. The book presents, in addition, some studies carried out in orthopedic and stomatological applications and others aiming to design and produce new devices using the latest advances in nanotechnology. This wide variety of theoretical, numerical and experimental results can help specialists involved in these disciplines to enhance competitiveness and innovation.

INTECH
open science | open minds

InTech Europe
University Campus STeP Ri
Slavka Krautzeka 83/A
51000 Rijeka, Croatia
Phone: +385 (51) 770 447
Fax: +385 (51) 686 166
www.intechopen.com

InTech China
Unit 405, Office Block, Hotel Equatorial Shanghai
No.65, Yan An Road (West), Shanghai, 200040, China
中国上海市延安西路65号上海国际贵都大饭店办公楼405单元
Phone: +86-21-62489820
Fax: +86-21-62489821

IntechOpen